7T Susceptibility Sensitive Imaging Detects Microarchitectural White Matter Differences Across the Healthy Corpus Callosum

Sharon K Schreiber[1], Bradley D Clymer[2], Michael V Knopp[3], and Petra Schmalbrock[3]

[1]*Biomedical Engineering, The Ohio State University, Columbus, Ohio, United States,* [2]*Electrical and Computer Engineering, The Ohio State University, Columbus, Ohio, United States,* [3]*Radiology, The Ohio State University, Columbus, Ohio, United States*

Introduction: High field (7T) susceptibility sensitive GRE MRI studies have repeatedly shown white matter (WM) heterogeneity suggestive of underlying neural architecture in both phase and magnitude images, although phase imaging was shown to produce better contrast [1-3]. Of the many mechanisms outlined for phase contrast, including susceptibility, chemical exchange with proteins, electronic screening effects, and sub-cellular magnetic architecture, Li has suggested that myelin susceptibility alone may be the dominant source [1]. Here we show that susceptibility simulations of the corpus callosum CC using an anatomical model of the CC [4,5] can reasonably predict experimentally measured parameters.

Methods: CC WM fibers were simulated as coaxial cylinders using a similar method as [5] based on detailed fiber distributions from [4], and g-factor (ratio of axon bundle caliber to fiber caliber) distributions from [6]. The simulated WM tracts (Figures 1 and 2) were constructed at the scale of actual voxel sizes (0.2 x 0.2 x 1 mm^3), but run in 2D (0.2 x 0.2) by taking advantage of the symmetry resulting from perpendicular alignment with respect to the main field. Using this set up, simulations were repeated for voxels for each region to estimate measured phase statistics. For this two compartment model, the susceptibility of myelin was approximated to be -9.23 ppm, the value listed for cholesterol which is a significant component of myelin, and the susceptibility used for CSF was -9.05 ppm [3]. Subvoxel field shifts were computed using an FFT method [7] and combined as complex exponentials to compute the total expected magnitude ($\sqrt{(R^2 + I^2)}$) and phase ($\tan^{-1}(I/R)$) shift for a single voxel imaged using a 7T GRE MRI sequence for TEs ranging from 5-25 ms. Repeat simulations for each voxel gave estimates for mean and variance, assuming uniform fiber distribution within a region, which is a fair assumption based on known histology [4].

Two CC data sets were collected. The first data set (Figure 3) used seven healthy human subjects (31-56y) imaged at 7T (Philips, Achieva) using a 16-channel receive coil (Nova medical) with the following acquisition parameters: 3D FFE sequence with TR/TE = 25/12 ms, flip angle = 5°, SENSE-factor = 2, acquisition voxel size = 0.4 x 0.68 x 1.6 mm^3, and axial slice orientation. The second data set (Table 1) focused on three males (34-31y) to avoid age and sex variability. This group was imaged using the same equipment with the following acquisition parameters: 3D FFE multi-echo sequence with TR/TE/ΔTE = 34 / 5 / 5 ms, flip angle = 5°, acquisition and reconstruction voxel size = 0.5 x 0.5 x 0.5 mm^3, SENSE=2, and sagittal slice orientation. For all subjects, imaging was only performed after signing an IRB approved-informed consent. Phase measurements were taken from images processed with our published HPF [8]. ROIs corresponding to genu, anterior body, midbody, posterior body, and splenium (Figure 2) comprising at least 30 independent voxels at an SNR of at least 10 were analyzed for mean phase, phase variance, and T2* measurements, and compared with simulation values as obtained above.

Results and Discussion: The results show that simulations using a simple two compartment coaxial cylinder model of the CC, where only susceptibility differences are taken into account, predict mean phase differences across the CC which are within a similar range as those measured within a group of healthy human subjects (Figure 3). This supports the idea that susceptibility is the dominant mechanism for phase contrast in the CC, as discussed by [1,2]. In addition, the T2* measurements from the simulation studies are comparable to experimentally measured values (Table 1). Furthermore, the simulations suggest that it might be possible to distinguish the different regional fiber architectures using T2* and phase statistics alone, as experimental measurement of T2* for a smaller than desirable population (three healthy males) suggests some regional statistical significance (ANOVA $p < 0.14$), and ANOVA analysis for both simulated and group measured regional phase variance statistics (dataset 1) shows more stringent statistical significance ($p < 0.0038$ and $p < 0.0446$ for simulated and group measured regional phase variances, respectively), at TE = 12 ms. We expect greater statistical significance when measuring group regional T2* with the inclusion of more healthy males, as the inter-subject variability increases the standard error, thus obscuring the true regional statistical significance which is more obvious for intrasubject regional analysis ($p < 10^{-10}$).

Conclusion: Simulated and experimental evidence suggests static susceptibility-weighted derived phase contrast can predominantly account for regional differences in mean phase across the CC. Similarly, regionally simulated T2* values are reasonably predictive of experimentally measured values. In addition, phase variance may be a useful parameter used in separating regional CC microstructure.

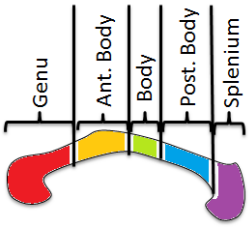

Figure 1: Diagram of the CC as divided into five combined regions, as described by [5]

Genu	Ant Body	Midbody	Post Body	Splenium
FVF=0.45	FVF=0.44	FVF=0.45	FVF=0.60	FVF=0.60
g=0.55	g=0.58	g=0.62	g=0.64	g=0.72

Figure 2: Two-compartment coaxial cylinder simulated models for the five regions of the CC

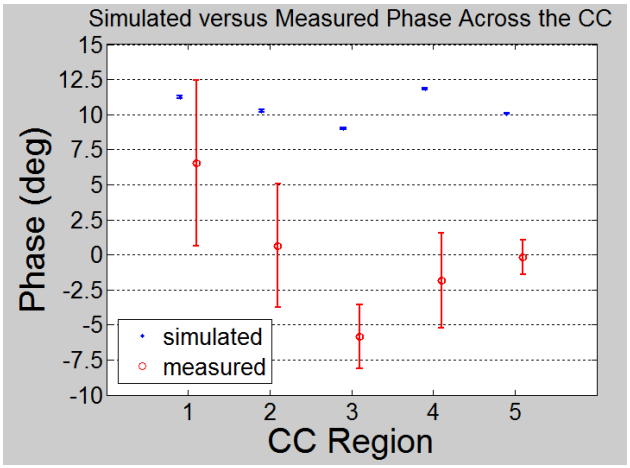

Figure 3: Between subject experimental and simulated mean phase at TE = 12 ms for healthy human subjects across the CC

	1	2	3	4	5
Experimental					
Subject 1	21.9±0.6	26.8±0.8	29.3±0.3	26.9±0.5	29.7±1.3
Subject 2	24.6±1.1	30.3±1.6	32.5±0.4	28.8±0.3	25.0±0.4
Subject 3	27.3±1.1	31.0±1.3	30.5±0.9	33.7±0.7	31.4±0.8
All subjects	25±3	29±2	31±2	30±4	29±3
Simulation	32.9±0.2	41.9±0.3	53.7±0.4	52.1±0.3	73.9±0.3
Literature[1]	21±3				29±2

Table 1: Experimentally measured and simulated T2* values across the CC (ms)

References: [1] Li, T.-Q. Mag Res in Med 62:1652-1657 (2009), [2] Li, T.-Q. NeuroImag 32:1032-1040 (2006), [3] Duyn, J.H. PNAS 104(28):11796-11801 (2007), [4] Aboitiz, F. Brain Res 598:143-153 (1992), [5] Stikov, ISMRM (2011), [6] Chatzopoulou, E. J. Neuroscience 28(30):7624-7636 (2008) , [7] Salomir, R. Concepts in Mag. Rs. Pt. B. 19B(1):26-34 (2003), [8] Abduljalil, A. J of Mag Res Img. 18:284-290 (2003)